Method of Measuring the Distance to an Object Based on One Shot Obtained from a Motionless Camera with a Fixed-Focus Lens

K. Murawski*
Military University of Technology, Institute of Teleinformatics and Automatics,
S. Kaliskiego 2, 00-908 Warsaw, Poland

(Received May 12, 2014)

The paper presents the method of measuring the distance to the object based on digital image processing. The solution is characterized in that the distance measurement to the object is performed by a motionless camera with established and unchanged parameters during measurement. The camera is equipped with a one non-stereoscopic lens. The measured distance is determined on the basis of one view of an object presented on one image. The image is made at a constant and invariant setting of the optical path such as: focus, aperture and focal length.

DOI: 10.12693/APhysPolA.127.1591
PACS: 06.30.Bp, 07.05.Pj, 07.07.Df

1. Introduction

The article presents a method of measuring the distance to an object through digital image processing. The image is acquired by a stationary camera equipped with a non-stereoscopic lens at a fixed focal length. The proposed solution is characterized in that in the course of conducting measurements all camera settings, including: focus, aperture and focal length as well as the camera position and the parameters of the optical path parameters remain unchanged. Only the position of the observed object is subject to modification.

Standard visional system for distance measurement comprises a light source and two video cameras forming a stereoscopic imaging system, Fig. 1a. By knowing the parameters of the cameras and their relative position, it is possible to determine the distance to the object [1]. Systems are presented in the literature for measuring the distance with one camera, Fig. 1b. The camera then operates in one of the four variants. In three of them, the camera takes a series of photos of the object (from two to eight [2]) in a system of moving camera or moving object. The distance is determined based on inverse perspective transformation after determining the characteristics of the object [3] and specifying its location on taken photos. The fourth case, Fig. 1c, applies to a camera with autofocus.

Such a camera is calibrated with standard parameters. Measuring the distance to the object involves taking sharp photos and calculating the distance using the lens equation [4–7]. Other methods of measuring the distance use the technique of light projection. Photogrammetry is one of them [1], including spectroscopical stereo photogrammetry [8]. Spectroscopic stereo photogrammetry allows achieving accurate measurement of distances of 0.02 mm [8]. A more popular method is the fringe projection technique [9–11]. In this method, the DLP projector or IR projects a known pattern of lines or system of points onto the observed object. The illuminated object is photographed and the resulting photo is subjected to digital image processing. The accuracy of the measurement obtained using this method reaches 0.5 mm [11]. Also common are distance measurement techniques, in which IR LED diodes, lasers [12–17], or acoustic sensors [18] are used. The distance is then determined based on measurements: the distance of the laser beam parallel to the optical axis of the camera from the centre of the recorded image [15], the time it takes the laser beam to reach and arrive back or the sound to/from an object [12, 13, 18–20], the characteristics of light traveling in an optical fiber woven into the structure of the observed and deforming material [16], laser beam intensity or the IR reflected from the surface of the object [21]. The listed techniques are characterized by high accuracy. However, the areas of their application are limited by: the speed of the automatic focus adjustment (autofocus), processing time, the range of the measured distance (up to 1 mm [8], up to 0.18 m [10], from 0.1 m to 1.8 m [15], from 0.2 m [11], from 1 m to 6 m [4], from 0.5 m to 100 m [13]); the required camera sensor resolution, the maximum number of processed frames per second (3008 px $\times$ 2000 px at 1 fps [4], 3248 px $\times$ 2160 px at 0.5 fps [15], 1280 px$\times$1024 px at 15 fps [8], 200 px$\times$200 px at 1.67 fps [11], 3 sensors $\times$ 64 px $\times$ 8 px at 100 fps [13]), and also the dimensions and weight of the sensor.

A large number of items of the literature prove that searching for other methods of measuring distances is intentional, especially for sensory applications. A high interest is observed in non-contact measurement techniques, simple solutions, a considerable operation speed, marginal measurement error and the possibility of miniaturising the sensor.

*e-mail: k.murawski@ita.wat.edu.pl

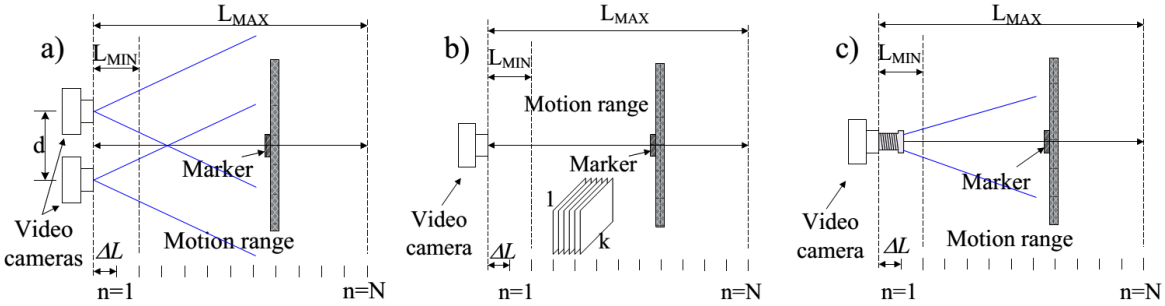

Fig. 1. Measuring the distance from the object using a camera.

The proposed method of measuring the distance to an object is an alternative to the solutions presented in the literature. Its main features are: operation in daylight, artificial light and infrared; no need to use complex systems generating structured light; determining the distance to objects close to the sensor (in the studies: from 0.07 m to 0.42 m); a small average of measurement error (in the studies: the average measurement error of moving the object relatively to the reference point equalled 1.32 mm); processing frames of the video signal at a high frequency (in the studies: 60 fps); determining the distance to the object at the frequency of incoming picture frames; the possibility of using lenses with a fixed focal length; contactless distance measurement carried out also in conditions of loss of focused images, low resolution image sensor (in the studies: 640 px × 480 px), a simple device design.

The limitations of the proposed method should include the necessity to place a marker on the object, to which the distance is measured, or indicating the area of the object that acts as a marker.

2. System configuration, image processing problem definition

The method of measuring the distance was studied using a camera with a CCD image sensor. The camera with dimensions of 42 mm × 32 mm and a weight of 5 g operated at a frequency of 60 fps and a resolution of 640 px × 480 px. The experiment was carried out in a setup as shown in Fig. 1c, with the exception that the camera was equipped with a HF16HA-1B lens with a fixed focal length. Distances indicated in Fig. 1c, equalled $L_{\min} = 0.07$ m, $L_{\max} = 0.42$ m. The measuring step ΔL was equal to 0.001 m and resulted from the use of a straight edge. A view of the measuring system is illustrated in Fig. 2.

The distance in the study was determined to the white plane (object) bearing a marker. The marker is a black circle with a diameter of $\varphi = 0.01$ m. Experiments were carried out in daylight and artificial light with a colour temperature of 2700 K generated by a CML-50 fluorescent tube. The resulting exemplary views of the marker: at maximum sharpness, reduced sharpness resulting from

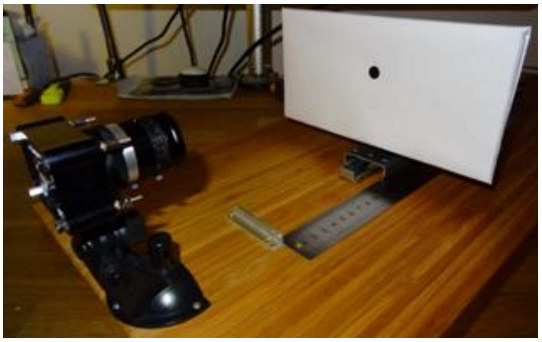

Fig. 2. View of the measuring system. Marker diameter is 0.01 m.

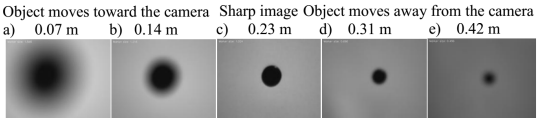

Fig. 3. An exemplary sequence of recorded images.

the close proximity of the object to the camera, and moving away from the marker, are shown in Fig. 3. The distances given in Fig. 3 were measured with a straight edge. The straight edge was situated parallel to the slider on which the object was mounted. The slider allowed the reproducibility of the conducted study, but did not provide coverage of the optical axis of the lens with the axis of the movement of the centre of gravity of the marker. Figure 4a presents profiles of horizontal lines of images determined by the centre of gravity of the marker for Fig. 3a (dashed line), Fig. 3c (continuous line), Fig. 3e (dotted line).

In Fig. 4a the marker movement can be observed in the horizontal plane as well as the change in intensity of pixels in the background (object) from approximately 200 for maximum close-up, to approximately 100 at the utmost distance of the object from the camera and the light source. The variability of the centre of gravity of the marker is shown in Fig. 4b. With the above a basic research problem arose of making the distance measurement result independent of: changes in levels of brightness, sharpness of acquired images, and the position of the marker in the area.

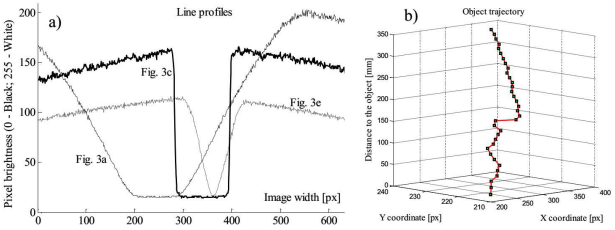

Fig. 4. Image line profiles determined by the centre of gravity of the marker: maximum close-up — dashed line, maximum level of sharpness — continuous line, maximum distance — dotted line (a), trajectory of the centre of gravity of the marker (b).

3. Distance measurement technique

The discussed measurement method, after calibration discussed further in Sect. 4, determines the distance to the object based on a single photo. The essence of the presented solution consists in the image analysis resulting from the object moving away from the position for which the focus was set. Figure 5 shows the profiles of the horizontal lines of the images (Fig. 3a, c, e) indicated by the centre of gravity of the marker as well as their behaviour during changes in distance from the marker. For the sharp marker view, Fig. 3c, sections AA′ and BB′ in Fig. 5 are almost vertical, which indicates a sharp cut-off of the view of the marker from the background. When the marker gets closer to the camera, the image becomes blurred, Fig. 3a. As a result, points A′ and B′ move respectively in the direction of A″ and B″. At the same time, the distance between points A and B remain almost unchanged. When the object with the marker moves away from the camera, points A″ and B″ return back to their initial position (A″ → A′, B″ → B′), and the image comes into focus again. Further distancing the object from the camera results in a repeated blurring of the image and the marker becoming smaller, Fig. 3e. In the case under consideration, the movement of points A → A‴ and B → B‴ is observed. The position of points A′ and B′ remain unchanged. The sequence of changes in the position of points A, A′, B, B′ determined during the object moving close and moving away from the camera with a step of $\Delta L = 0.01$ m is presented in Fig. 6. Changing the position of points A, A′, B, B′ are presented in Fig. 5 and Fig. 6 was used to determine the distance to the object. For this purpose, the image from the camera underwent defuzzification. Defuzzification was performed using image binarisation with a threshold T_{H} equal to 70. The selection of binarisation consists in determining such a T_{H} value to obtain a uniform distribution of points intersecting profile image horizontal lines (indicated by the centre of gravity of the marker) with the line illustrating the tested value T_{H}, Fig. 6. The location of the determined points are unambiguously associated with the distance d of the marker from the camera (see Table I).

The distribution of points is described by the equation in the calibration process. The result is a relation

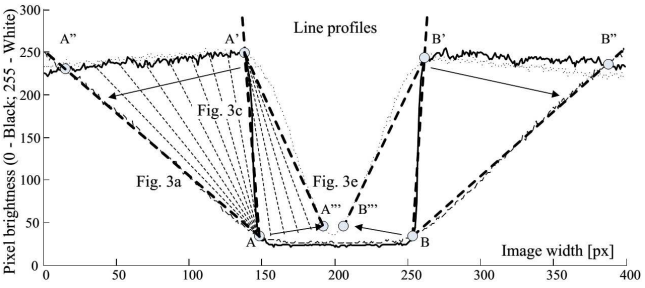

Fig. 5. Horizontal line profiles for images from Fig. 3a, c, e determined by the centre of gravity of the object after standardising brightness.

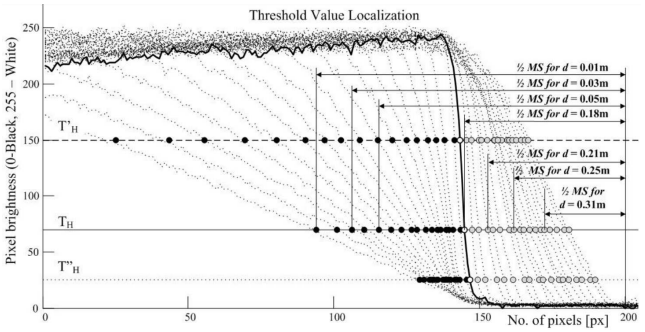

Fig. 6. Distribution of essential points due to determining the distance to the object for the accepted threshold value T_{H} at $L_{\min} = 0.07$ m, $L_{\max} = 0.42$ m and $\Delta L = 0.01$ m.

TABLE I

Relative change in marker size MS as a function of distance from the camera.

d	MS			d	MS		
[m]	Min.	Mean	Max.	[m]	Min.	Mean	Max.
0.35	0.432	0.457	0.488	0.17	0.968	0.968	0.968
0.34	0.456	0.475	0.496	0.16	0.992	1.000	1.000
0.33	0.472	0.492	0.520	0.15	1.016	1.023	1.024
0.32	0.496	0.511	0.536	0.14	1.040	1.041	1.048
0.31	0.520	0.534	0.552	0.13	1.056	1.061	1.064
0.30	0.536	0.553	0.576	0.12	1.072	1.080	1.088
0.29	0.560	0.573	0.592	0.11	1.096	1.101	1.112
0.28	0.584	0.595	0.616	0.10	1.112	1.121	1.136
0.27	0.608	0.622	0.632	0.09	1.128	1.147	1.160
0.26	0.640	0.647	0.656	0.08	1.160	1.172	1.184
0.25	0.664	0.674	0.688	0.07	1.192	1.203	1.224
0.24	0.696	0.704	0.712	0.06	1.224	1.240	1.264
0.23	0.728	0.735	0.744	0.05	1.256	1.276	1.296
0.22	0.768	0.769	0.784	0.04	1.288	1.314	1.344
0.21	0.800	0.806	0.816	0.03	1.336	1.361	1.400
0.20	0.840	0.842	0.856	0.02	1.384	1.414	1.456
0.19	0.880	0.882	0.896	0.01	1.440	1.481	1.528
0.18	0.928	0.928	0.928	0.001	1.528	1.567	1.632

where d — offset from $L_{\min}$,
MS — measured relative change in marker size.

that describes the object distance from the camera as a function of changes in the size of the marker.

4. Calibration procedure

The calibration procedure was carried out in the configuration shown in Fig. 1c. In the study the values $L_{\min}$, $L_{\max}$ and ΔL equaled: 0.07, 0.42, and 0.01 m. The distance was determined to the white plane (object) with a black circle (marker) with a diameter of $\varphi = 0.01$ m. The sharpness of the image was set from a distance of 0.23 m. The width of the marker was expressed in px as well as measurement step. Measurement step was calculated by dividing one by the width of the marker, which is measured in pixels. The width of the marker was determined in pixels as well as the measurement step. The measurement step was calculated as 1/the width of the marker measured in pixels. For each position of the plane with an offset relative to $L_{\min}$ by d (see Table I), a series of 1000 measurements of the width of the marker were performed. The mean value was calculated from these measurements and the minimum and maximum value was determined. The resulting values

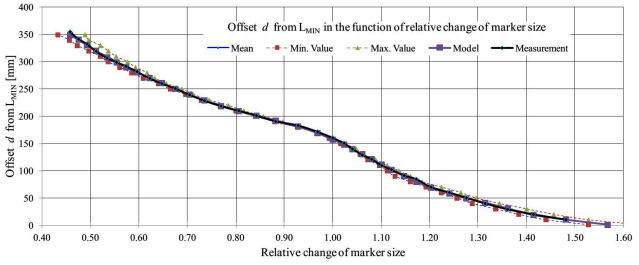

Fig. 7. Distance characteristic to the plane in the function of changes in marker size.

multiplied by the measurement step are included in Table I. The values of parameter d expressed as a function of MS is presented in Fig. 7. The characteristic presented in Fig. 7 was described with a polynomial model in the form of

$$f(V,\mu,\sigma,x) = v_{10}z^{10} + v_9z^9 + v_8z^8 + v_7z^7 + v_6z^6$$
$$+v_5z^5 + v_4z^4 + v_3z^3 + v_2z^2 + v_1z^1 + v.$$

Symbols used in the model represent: $z = (x-\mu)/\sigma$; μ — average from measurements: 0.92688; σ — standard deviation from measurements: 0.31737; $V = \langle v_{10}, v_9, v_8, v_7, v_6, v_5, v_4, v_3, v_2, v_1, v_0\rangle$, where $v_{10} = -4.3621$, $v_9 = 8.3989$, $v_8 = 28.7860$, $v_7 = -49.1840$, $v_6 = -77.3800$, $v_5 = 100.2900$, $v_4 = 112.2500$, $v_3 = -83.5540$, $v_2 = -74.6610$, $v_1 = -85.0020$, $v_0 = 181.5500$.

Adjusting the model "Model" to the measurement results "Measurement" was presented in Fig. 7. For the determined model the norm of residuals equalled 6.7852 mm. The average error of distance determination based on the model for average marker size equalled 0.96 mm.

The presented calibration procedure is performed only once.

5. Results of research

The presented method of measurement was verified by measuring the distance to the moving objects. The objects were marked with a marker. The marker was a black circle with a diameter of $\varphi = 0.01$ m drawn on a white background. The measurement step was determined as 1 divided by the width of the marker measured in pixels. The calculated measurement step equalled 0.008.

The study was carried out using a station as the one shown in Fig. 2. Artificial light produced by a CML050 fluorescent tube was used as a light source.

TABLE II

Values of offset d determined based on measurements.

d	VoM	δ		d	VoM	δ	
[mm]	[mm]	[mm]	[%]	[mm]	[mm]	[mm]	[%]
350	355.23	5.23	1.494	170	171.79	1.79	1.053
340	342.10	2.10	0.618	160	160.47	0.47	0.294
330	333.19	3.19	0.967	150	150.77	0.77	0.513
320	319.66	3.4	0.106	140	140.19	0.19	0.136
310	307.11	2.89	0.932	130	128.97	1.03	0.792
300	299.44	0.56	0.187	120	121.30	1.30	1.083
290	292.28	2.28	0.786	110	109.79	0.21	0.191
280	282.23	2.23	0.796	100	102.27	2.27	2.270
270	269.58	0.42	0.156	90	91.50	1.50	1.667
260	260.35	0.35	0.135	80	84.77	4.77	5.963
250	251.29	1.29	0.516	70	70.00	0.00	0.000
240	239.62	0.38	0.158	60	60.36	0.36	0.600
230	228.76	1.24	0.539	50	50.52	0.52	1.040
220	219.03	0.97	0.441	40	40.15	0.15	0.375
210	210.56	0.56	0.267	30	29.36	0.64	2.133
200	201.39	1.39	0.695	20	20.12	0.12	0.600
190	191.02	1.02	0.537	10	10.42	0.42	4.200
180	183.36	3.36	1.867				

where d — offset from $L_{\min}$,
VoM — value of measurement, δ — measurement error.

In the experiment d was adopted (offset from $L_{\min}$) in the range of 0.01 m to 0.35 m. The sharpness of the images was set at a distance of 0.23 m. The results of measurements are included in Table II. In the presented example, the distance to the object is calculated from the equation $L_{\min} + d$. The average measurement error of the d offset equaled 1.32 mm (0.97%). Given that $L_{\min}$ was equal to 0.07 m, the distance to the object were determined with an average measurement error equal to 0.54%.

6. Conclusions

Studies have shown that on the basis of the image of the initially known marker the motionless camera equipped with a fixed focal length lens can determine the distance to a moving object. Measuring distances in meters requires a one-time calibration of the measurement system. The average measurement error of the d marker shifting for the camera (640 px × 480 px) used in the conducted experiments in daylight and artificial light for the

distances of 0.07 m to 0.42 m was 1.32 mm (0.97%). Taking to account that $L_{\min} = 0.07$ m the average distance measurement error to the object was 0.41%. The presented technique was used to measure the amplitude and frequency of vibration of the flat membrane as well as the construction of a video-manometer. According to the author, this technique can also be used in control systems with video feedback, control and data transferring systems using the phenomenon of image blur as well as object tracking systems of different classes [22, 23].

Acknowledgments

The author would like to thank Prof. Tadeusz Pustelny as well as Ph.D. Eng. Grzegorz Konieczny from the Silesian University of Technology, whose publications have been an inspiration to this work.

The work was presented at the 8th Conference Integrated Optics — Sensors, Sensing Structures and Methods, IOS'2014 sponsored by Polish Academy of Sciences. The conference was organized by the Committee of Electronics and Telecommunication at the Polish Academy of Sciences in cooperation with the Upper Silesian Division of the Polish Acoustical Society and Photonic Society of Poland, as well as the Department of Optoelectronics at the Silesian University of Technology.

References

[1] http://tdserver1.fnal.gov/darve/mu_cool/pressuretest/Basics_of_Photogrammetry.pdf, (2014).

[2] K. Różanowski, K. Murawski, *Acta Phys. Pol. A* **122**, 874 (2012).

[3] K. Murawski, K. Różanowski, *Acta Phys. Pol. A* **124**, 509 (2013).

[4] A. de La Bourdonnaye, R. Doskočil, V. Křivánek, A. Štefek, *Adv. Milit. Technol.* **7**, 2 (2012).

[5] K. Różanowski, K. Murawski, *Acta Phys. Pol. A* **124**, 558 (2013).

[6] K. Murawski, *Przegląd Elektrotechniczny* **9**, 184 (2010) (in Polish).

[7] K. Murawski, in: *Proc. XV Int. Conf. on Methods and Models in Automation and Robotics (MMAR), Międzyzdroje (Poland)*, Ed. Z. Emirsajłow, 2010, p. 356.

[8] K. Yue, Z. Li, M. Zhang, S. Chen, *Opt. Expr.* **18**, 26866 (2010).

[9] G. Hong, Ph.D. Thesis, Stony Brook University, 2009.

[10] Y. Morimoto, A. Masaya, M. Fujigaki, D. Asai, *Applied Measurement Systems*, 2012, Ch. 7, p. 137.

[11] C. Matabosch, D. Fofi, J. Salvi, J. Forest, *LNCS* **3522**, 145 (2005).

[12] T. Sondej, R. Pelka, in: *Proc. IEEE Int. Conf. on Computational Intelligence for Measurement Systems and Applications*, 2004, p. 181.

[13] B. Konig, Ph.D. Thesis, Universitat Duisburg-Essen, 2008.

[14] J. Kramer, P. Seitz, *Sens Actuat. A* **31**, 241 (1992).

[15] T. Wang, M. Lu, W. Wang, C. Tsai, in: *Proc. 7th WSEAS Int. Conf. on Signal Processing, Computational Geometry and Artificial Vision*, 2007, p. 1.

[16] B. Glisic, D. Inaudi, P. Kronenberg, S. Lloret, S. Vurpillot, in: *Proc. SPIE 6th Int. Symp. on Smart Structures and Materials*, 1999, p. 1.

[17] G. Konieczny, T. Pustelny, *Acta Phys. Pol. A* **122**, 962 (2012).

[18] G. Konieczny, Z. Opilski, T. Pustelny, *Acta Phys. Pol. A* **120**, 688 (2011).

[19] G. Konieczny, T. Pustelny, P. Marczyński, *Acta Phys. Pol. A* **124**, 479 (2013).

[20] G. Konieczny, T. Pustelny, P. Marczyński, *Acta Phys. Pol. A* **124**, 483 (2013).

[21] K. Murawski, R. Różycki, P. Murawski, A. Matyja, M. Rekas, *Acta Phys. Pol. A* **124**, 517 (2013).

[22] G. Konieczny, Z. Opilski, T. Pustelny, E. Maciak, *Acta Phys. Pol. A* **116**, 344 (2009).

[23] K. Murawski, K. Różanowski, M. Krej, *Acta Phys. Pol. A* **124**, 513 (2013).